

# Combining Interferometric Radar and Laser Altimeter Data to Improve Estimates of Topography

K. Clint Slatton<sup>1,3</sup>, Melba M. Crawford<sup>1,2</sup>, and Brian L. Evans<sup>3</sup>

<sup>1</sup>Center for Space Research, The University of Texas at Austin  
3925 W. Braker Ln., Suite 200, Austin, TX 78759-5321

<sup>2</sup>Dept. of Mechanical Engineering, The University of Texas at Austin

<sup>3</sup>Dept. of Electrical and Computer Engineering, The University of Texas at Austin

E-mail: slatton@csr.utexas.edu, Ph: +1.512.471.5509, Fax: +1.512.471.3570

Abstract -- Interferometric synthetic aperture radar (INSAR) has been used to map terrain topography; however, accuracy is limited because observations are not measurements of true surface topography over vegetated areas. Instead, the measurements, which depend on the sensor and the vegetation, represent some height above the true surface. We solve an inverse problem for INSAR scattering to determine surface and vegetation elevations, and then incorporate sparse laser altimeter observations to improve the estimates of surface and vegetation elevations.

## 1. INTRODUCTION

There is a critical need to measure land surface topography over large areas to assess the threat and impact of natural hazards such as flooding. Imaging radars have been used extensively to map terrain because they can operate in the microwave portion of the electromagnetic spectrum, thereby enabling them to image during the day or night and under most weather conditions. Interferometric and stereo synthetic aperture radar (SAR) data can be used to determine topography over large areas, but interferometric SAR (INSAR) data provide the best option for making primary topographic measurements in low-relief areas.

Although topographic mapping with INSAR has been demonstrated, success has been generally limited to areas where the surface is not obscured by significant vegetation [1]. For many applications, topographic features of interest occur in heavily vegetated regions, such as forests. INSAR observations do not provide direct measurements of the true surface topography in vegetated areas, but instead yield a height  $z_s$  that depends on the sensor characteristics, the surface elevation  $z_g$ , and the vegetation height  $z_v$ .

Vertical height accuracies of 2–5 m can be obtained in non-vegetated regions with airborne INSAR data processed to 10 m  $\times$  10 m terrain patches (pixels), but the presence of vegetation can lead to errors in the computed surface topography of tens of meters in forested areas. A method is needed to distinguish surface elevations  $z_g$  and vegetation heights  $z_v$  from  $z_s$ . One approach is to develop a functional relationship relating the INSAR observations

to  $z_g$  and  $z_v$  using an electromagnetic scattering model [2]. Estimating the parameters  $z_g$  and  $z_v$  from the observations is then equivalent to inverting the model. Unfortunately, baseline constraints and the sensitivity of the INSAR to various terrain parameters often lead to unacceptably large variances of the estimates. Combining INSAR with laser altimetry (LIDAR) can improve the accuracy of the INSAR-derived estimates. In this paper, a method for integrating LIDAR observations with INSAR-derived estimates of surface and vegetation elevations is presented. The LIDAR information can be propagated into the INSAR estimates beyond the location of the LIDAR observation.

## 2. INSAR ESTIMATION

Over barren surfaces, the phase difference used to determine  $z_s$  has a relatively small variance dictated by measurement noise. Over vegetated terrain, the INSAR signal can scatter from both the ground surface and vegetation constituents, e.g. tree trunks and branches. Therefore, the value of  $z_s$  cannot be related to the physical topography or vegetation heights from the phase data alone. Analytical scattering models can be used to relate  $z_s$  to certain target parameters. If the scattering model does not have a closed-form inverse, it can be effectively inverted by formulating an estimation problem. INSAR observations from two baselines are used to recover a minimal set of terrain parameters: surface elevation  $z_g$ , vegetation height  $\Delta z_v$ , and extinction coefficient  $\tau$ .

In this study, we implement the scattering model developed in [2], and invert it using nonlinear constrained optimization methods [3]. The model is of the form  $\mathbf{A}(\mathbf{x}) = \mathbf{b}$ , where  $\mathbf{b}$  is a  $4 \times 1$  vector of dual-baseline observations,  $\mathbf{A}$  is the nonlinear scattering model, and  $\mathbf{x}$  is a  $3 \times 1$  vector of the terrain parameters. The function  $\min f(\mathbf{x})$  is minimized subject to inequality constraints  $g(\mathbf{x})$  that bound the feasible region for the values of  $\mathbf{x}$  (1). Here,  $f(\mathbf{x})$  is the sum of squared errors between the observations and the model (2).

$$\min f(\mathbf{x}), \text{ subject to } g(\mathbf{x}) \leq \mathbf{0} \quad (1)$$

$$f(\mathbf{x}) = \|\mathcal{A}(\mathbf{x}) - \mathbf{b}\|_2^2 \quad (2)$$

INSAR and LIDAR data were acquired over a test site on the Texas coast. C-band ( $\lambda = 5.7$  cm) INSAR data were acquired by the NASA/JPL Airborne SAR (AIRSAR) sensor. The Optech, Inc. Airborne Laser Terrain Mapping (ALTM) system acquired laser altimetry data at  $\lambda = 1047$  nm. LIDAR and single-baseline INSAR data were processed for the test site and analyzed in [3]. However, the dual-baseline INSAR data from the test site have not yet been processed. Therefore, simulated data are used here to investigate the incorporation of LIDAR observations into the INSAR estimation procedure.

It was found that inverting the model in [2] provided good estimates of the vegetation height  $\Delta\hat{z}_v$  in virtually all cases. Estimates of ground elevation  $\hat{z}_g$  were much more dependent on the height of the vegetation. Using LIDAR data, we were able to improve the  $\hat{z}_g$  estimates.

### 3. LIDAR DATA

LIDAR sensors typically scan through a small angle about the nadir direction. Footprint patterns are generally dense swaths, many of which are required for wide-area coverage. LIDAR sensors can resolve vegetation and topography better than INSAR in both the horizontal and vertical dimensions. This is due to the small footprint of the laser and minimal penetration of the canopy at the optical wavelengths used in LIDAR. Typical vertical accuracy for single-pass airborne INSAR is 2-5 m over level, non-vegetated terrain, with 10 km imaging swaths. LIDAR systems can yield 10 cm vertical accuracy, but imaging swaths are generally less than 0.5 km, thereby requiring extensive gridding and removal of interflightline effects for development of a DEM. For extensive areas, a DEM based totally on LIDAR is impractical. However, LIDAR has potential as a complementary measurement to INSAR.

The LIDAR data used in this study were gridded into a regular-spaced lattice with 10 m postings to match the resolution of the INSAR data. This posting is much larger than the original LIDAR pulse spacing, so the standard deviation of the LIDAR heights that contributed to each gridded pixel  $\sigma_L$  was computed. In vegetated areas, LIDAR is primarily sensitive to the absolute height of the vegetation, but surface heights can be measured where there is minimal vegetation cover. When dense wide-area coverage data are available, it is possible to discern barren from vegetated areas in the  $z_L$  imagery. In the nominal case of sparse coverage, it is still possible to discern barren from vegetated areas using  $\sigma_L$  imagery.

Analysis of LIDAR data over the test site indicated that a simple threshold-based classification using  $\sigma_L$  data identifies nearly barren and vegetated areas. Barren and grass-covered areas were considered as minimally vegetated, where  $z_L \approx z_g$ . Where there is minimal vegetation, adjacent LIDAR pulses scatter off the ground surface, yielding a low standard deviation of heights for that pixel. Over significant vegetation, some LIDAR pulses scatter from the highest parts of the canopy, while other pulses penetrate into the top layer, so the standard deviation of the data is higher. Standard deviations between 0.1 m and 5.0 m were observed over the test site. An empirically determined threshold value of 0.4 m provided the best separation between tall vegetation, such as trees and shrubs, and minimally-vegetated areas, although values between 0.2 m and 0.7 m were also adequate.

### 4. COMBINING DATA TYPES

Values given in [2] for measurement noise of dual-baseline INSAR observations over non-vegetated areas were applied to the simulated INSAR observations. An additive, zero-mean, white Gaussian process was used to model height errors not attributable to vegetation [4]. Although uniform distributions are often used to model phase noise, Gaussian distributions are appropriate for height errors due to phase-difference noise [5], [6].

Although dense LIDAR coverage was available over the test site, a more conservative LIDAR acquisition was assumed for the simulation. A single LIDAR swath approximately in the azimuth direction of the INSAR imaging swath could provide  $\sigma_L$  measurements for each range line in the SAR image. The availability of  $\sigma_L$  at each LIDAR pixel is consistent with a single imaging swath and a pulse density achieved with the ALTM.

2-D arrays of ground elevations and vegetation heights were specified and used to generate noisy dual-baseline INSAR observations using the scattering model in [2]. Various deterministic trends plus random variations were investigated to simulate realistic terrain and vegetation. LIDAR information was used where  $\Delta z_v \leq 0.8$  m in the simulation, corresponding approximately to  $\sigma_L < 0.4$  in the actual data. Only two LIDAR samples were allowed per SAR range line to represent limited LIDAR coverage. At these samples, the estimate for the ground elevation was replaced by the LIDAR height.

Using the LIDAR at specific samples improved the estimates at those samples. It also tended to improve the subsequent estimates because the previous estimate is used as the initial guess for the current estimate. The LIDAR was then more systematically propagated in areas of minimal vegetation by making the estimates of pixels

adjacent to the LIDAR sample linear combinations of the current estimate and the adjacent LIDAR measurement. LIDAR data over minimally vegetated areas exhibited correlation lengths  $\geq 3$  pixels (30 m), with less correlation over vegetated areas. As a compromise, the support of the weighting function was extended over one pixel to either side of the LIDAR sample. The weights assigned to the current estimate and adjacent LIDAR-supplied value, were 0.6 and 0.4 respectively. The weights were chosen to have a low-pass structure for smoothing.

## 5. RESULTS

Table 1 shows the mean absolute errors and maximum absolute errors between the estimates and true values for ground elevations and vegetation heights. Including LIDAR observations reduced both the average and maximum errors. Propagating the LIDAR reduced the error further. Most of the improvement is in the ground elevations, as expected. Figure 1 shows true ground elevations versus estimated ground elevations in the propagated LIDAR case. These results were obtained with  $\Delta z_v$  ranging from 0.2 m to  $>6$  m and incidence angles near  $35^\circ$  to  $40^\circ$ .

Table 1. Estimate errors: mean absolute error (MAE) and maximum absolute error (MxE).

MAE	$z_g$ (m)	$\Delta z_v$ (m)
No LIDAR	0.49	0.05
LIDAR	0.47	0.05
Propagated LIDAR	0.38	0.04
MxE	$z_g$ (m)	$\Delta z_v$ (m)
No LIDAR	2.55	0.66
LIDAR	2.07	0.57
Propagated LIDAR	1.50	0.42

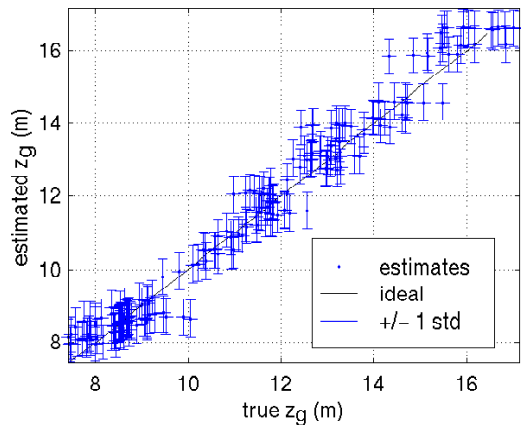


Figure 1. Scatter plot of  $z_g$  for propagated LIDAR

## 6. CONCLUSIONS

A method for incorporating LIDAR data to improve INSAR-derived estimates of terrain parameters was developed, and initial results show promise. LIDAR was first used only at a sparse set of locations where the vegetation cover was minimal. This significantly improved  $\hat{z}_g$  at the corresponding samples. The LIDAR information was then propagated to adjacent pixels, improving results further.

Although current results are only preliminary, a structure is in place to further study the problem. Several terrain scenarios were considered in the simulations, but much more will be learned when the dual-baseline INSAR data are processed and the algorithms are applied to real data. The INSAR-derived estimate errors will probably increase when applied to actual data, but the impact of the LIDAR may be greater.

## 7. ACKNOWLEDGEMENTS

This work was supported by the National Aeronautics and Space Administration, under the Graduate Student Research Fellowship Program (Grant NGT-50239), the United States Army (Grant DAAG55-98-1-0287), and the Jet Propulsion Laboratory (Grant 961381).

## 8. REFERENCES

- [1] F. Li and R. M. Goldstein, "Studies of multi-baseline spaceborne interferometric synthetic aperture radars," *IEEE Trans. Geosci. Remote Sensing*, vol. 28, no. 5, pp. 88-97, 1990.
- [2] R. N. Treuhaft and P. R. Siqueira, "Vertical structure of vegetated land surfaces from interferometric and polarimetric radar," *Radio Science*, vol. 35, no. 1, pp. 141-177, 1999.
- [3] K. C. Slatton, M. M. Crawford, B. L. Evans, "Improved Accuracy for Interferometric Radar Images Using Polarimetric Radar and Laser Altimetry Data," *Proc. IEEE Southwest Symposium On Image Analysis and Interpretation*, April 2-4, 2000, pp. 156-160.
- [4] J. O. Hagberg, L. M. Ulander, and J. Askne, "Repeat-pass SAR interferometry over forested terrain," *IEEE Trans. Geosci. Remote Sensing*, vol. 33, no. 2, pp. 331-40, 1995.
- [5] J. S. Lee, K. P. Papathanassiou, T. L. Ainsworth, M. R. Grunes, and A. Reigber, "A new technique for noise filtering of SAR interferogram phase images," *Proc. IEEE Int. Geosci. Remote Sensing Symp.*, Singapore, pp. 1716-18, 1997.
- [6] N. P. Nikolous and E. H. Meier, "First results with airborne single-pass DO-SAR interferometer," *IEEE Trans. Geosci. Remote Sensing*, vol. 33, no. 5, pp. 1230-7, 1995.